Soft Sediments: Wave-based Characterization

Katherine Klein[1] and J. Carlos Santamarina[2]

Abstract: Soft sediments are frequently encountered in geotechnical practice, forming natural deposits or manmade mixtures. These high water content soil–water mixtures involve soils with high specific surface and experience relatively low effective stresses, hence the role of electrical interparticle forces is enhanced and nonstandard soil-like behavior may be observed. Testing such materials presents some unique challenges not faced in soils with a stronger granular skeleton. This experimental study of soft sediments involves kaolinite–electrolyte mixtures. Two test sets are conducted. The first one involves index tests and the second set of tests explores the combined utilization of elastic and electromagnetic waves to assess soft sediments and to monitor their evolution. The kaolinite mixtures tested in both sets of measurements were prepared using fluids of different ionic concentrations to create different soil fabrics. The mixtures change behavior when the ionic concentration of NaCl exceeds ~0.1 mol/L, indicating internal changes in fabric formation. While the liquid limit is sensitive to fluid–particle interactions, it is less sensitive to fabric effects than viscosity or sedimentation tests. The maximum porosity a soil may attain is determined by the particle slenderness; in the case of kaolinite, a skeleton capable of transmitting a shear perturbation is observed at water content as high as six times the liquid limit. At this incipient skeletal condition, minor differences in shear wave velocity hint to the stiffness of different fabrics. High frequency permittivity is a good indicator of water content and can be effectively used to monitor the evolution of soft sediments. On the other hand, the evolution of the effective conductivity varies with pore fluid concentration: for high ionic concentration fluids, the effective conductivity increases as porosity increases, yet, the opposite is true for low ionic concentration fluids due to the contribution of surface conduction. In a wide range of water contents [0.6 liquid limit (LL) $<w<$ 6 LL], the shear wave velocity is primarily determined by the water content or porosity, and fabric appears to have a limited impact. Test procedures and results can be used to develop parallel field characterization tools and interpretation guidelines.

DOI: 10.1061/(ASCE)1532-3641(2005)5:2(147)

CE Database subject headings: Electrical conductivity; Shear waves; Sediment; Sedimentation; Fabric; Slurries; Viscosity.

Introduction

"Soft sediments" refer to deposits with a high water content (near or above the liquid limit), where the percolating skeleton is made of fine-grained soils (clay fraction above ~20%), with a high degree of saturation, and subjected to low effective confinement. Soft sediments and their related implications are frequently encountered in underwater geotechnics (fluvial, lacustrian, or marine deposits; dredging operations; erodability; and stability of foundations underwater), on-shore construction (cut-off walls, drilling muds, hydraulic-fill, flowable fill), and mining (processing, waste disposal, tailing ponds, stable distribution of mining products such as latex paints and paper coating slurries).

The study of soft sediments has often been cast in the context of the sedimentation behavior of soft slurries and the understanding of mechanisms that contribute to the early induction period, hindered settlement, consolidation, secondary consolidation, aging, and associated thixotropic effects (see for example Work and Kohler 1940; Kynch 1952; Richardson and Zaki 1954; McRoberts and Nixon 1976; Been and Sills 1981; Tiller and Khatib 1984; Zreik et al. 1997). Such studies have shown that a unique relationship between void ratio and effective stress does not exist in soft sediments; that is, a soil layer with a given water content can exist in equilibrium under different effective stresses (Been and Sills 1981; Zreik et al. 1997). Furthermore, thixotropic effects enhance the stability of the soft sediments in time.

In high water content sedimentation tests, three different regimes or conditions can be identified (Fig. 1): (1) the "suspension" condition where particles do not form a skeleton capable of transmitting a shear perturbation (effective skeletal stress $\sigma'=0$ and shear stiffness $G=0$); (2) the "soft sediment" condition, which is a transition stage between the suspension phase and the soil phase, where the properties of the percolating granular skeleton are determined by long-range interparticle electrical forces ($\sigma'=0$ and $G>0$); and (3) the "Terzaghian soil" condition where behavior is determined by interparticle skeletal forces that result from applied effective stresses ($\sigma'>0$ and $G>0$). Been and Sills (1981) hypothesize that the transition stage is where the flocs in suspension come into contact with each other and start breaking up. Then, as more particles settle, the weight of the overlying particles decreases the interparticle distances and a soil forms (Sridharan and Prakash 1998). Soil formation occurs due to particle movement and possibly due to a reorganization of the water structure, both of which are time dependent processes (Zreik et al. 1997). Thus, the accumulation rate of sedimenting particles is faster than the construction rate of the soil structure, resulting in creep (Toorman 1999).

The concept of interparticle contact becomes fuzzy in the case

[1]Assistant Professor, Univ. of Toronto, Toronto, Ontario, Canada M5S 1A4. E-mail: klein@civ.utoronto.ca

[2]Professor, Georgia Institute of Technology, Atlanta, GA 30332-0355. E-mail: carlos.santamarina@ce.gatech.edu

Note. Discussion open until November 1, 2005. Separate discussions must be submitted for individual papers. To extend the closing date by one month, a written request must be filed with the ASCE Managing Editor. The manuscript for this paper was submitted for review and possible publication on February 18, 2004; approved on October 25, 2004. This paper is part of the ***International Journal of Geomechanics***, Vol. 5, No. 2, June 1, 2005. ©ASCE, ISSN 1532-3641/2005/2-147–157/$25.00.

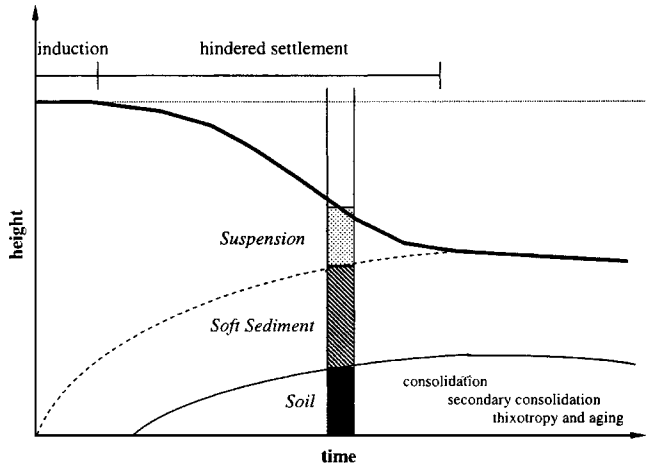

Fig. 1. Sedimentation of high water content slurries. Three mixture conditions: suspension ($\sigma' = 0$ and $G = 0$), soft sediment ($\sigma' = 0$ and $G > 0$), and soil ($\sigma' > 0$ and $G > 0$)

of fine particles and high water contents. In a very general sense, two particles are "in contact" when there is an interaction between them. Two particles in very close proximity interact through Born repulsion and hydration forces (separation distance less than 10^{-9} m). Long-range electrical forces can extend to about 10^{-8} m. Furthermore, particles can interact through hydrodynamic effects to a distance on the order of the particle diameter (Esquivel-Sirvent et al. 1995).

Studies have shown that a significant change in the yield stress of slurries occurs at water contents 1.4–2.5 times the liquid limit (kaolinite and till; mixtures of illite, smectite, and kaolinite) (Inoue et al. 1990; Fakher et al. 1999). This change would indicate the development of effective stress and the transition from a soft sediment to a soil. In fact, Zreik et al. (1997) found that shear strength is related to water content in young specimens soon after the soil skeleton is formed, and it becomes effective stress dependent as time elapses. Large amplitude disturbance during fabric formation affects the final structure of the soil and renders sediments with lower stability at the same water content (Zreik et al. 1997). On the other hand, small amplitude vibrations can enhance the formation of a stable skeleton (rheopexy) (van Olphen 1977).

Clearly, the behavior of soft sediments presents intriguing differences with respect to the more typical soils encountered in geotechnical practice. Even a cursory examination soon renders questions in relation to the nature of particle contacts, the suspension-to-sediment-to-soil transition, and the role of initial fabric on behavior. The purpose of this study is to enhance the understanding of soft sediments, taking into consideration the governing interparticle forces, conditions that render different fabrics such as depositional environment and remolding, and differences in water content. Given the inherent experimental difficulties related to the study of undisturbed soft sediments, this study places emphasis on wave-based measurements, using both low energy electromagnetic and elastic shear waves. This paper begins with a particle-level interpretation of soft sediments and fabric formation. Then, a two part experimental study is documented.

Soft Sediments at Microscale: Interparticle Forces and Fabric

The common characteristics of soft sediments listed previously, "saturated, clay-size particles at low confinement," point to the balance between underlying governing forces. These conditions imply that capillary interparticle forces are absent, and that both the weight of the particles and the skeletal forces that result from the applied effective stresses are small relative to the interparticle electrical forces. This is a particle-level, fundamental definition of soft sediments. Indeed, when interparticle forces are computed, results show that van der Waals attraction can overcome the particle weight for particles smaller than ~ 10 μm (computations and additional guidelines can be found in Santamarina 2003).

Since electrical forces exceed the weight of individual particles, the development of particle associations and fabric formation is determined by interparticle attraction and repulsion forces. The following key physical phenomena form the basis for the interpretation of fabric formation:

1. Crystal boundaries, isomorphic substitution and structural defects, give clay particles a structural charge (Velde 1992; Weaver 1989).
2. The "effective charge" of a particle is not an inherent quantity, but depends on the measurement method and pH (dissolution, protonation, and deprotonation). The isoelectric point (IEP) is the pH at which the zeta potential is zero (Sposito 1998).
3. The structural differences on edge and face surfaces imply different sensitivities of the edges and faces to protonation and complexation. Therefore, different isoelectric points for edges and faces can be distinguished (Williams and Williams 1978).
4. The lower the ionic valence and concentration in the pore fluid, the thicker the diffuse double layer and the greater the interparticle repulsion at a given interparticle distance. On the other hand, high ionic valence and/or concentration reduce the Stern potential and shrink the double layer (Mitchell 1993; Lyklema 1995).
5. The van der Waals attraction depends on the permittivity of the pore fluid (Hamaker constant) and is little affected by ionic concentration (Israelachvili 1992).
6. The association of two particles reflects the governing interparticle forces. Three minimum energy particle associations are commonly recognized (van Olphen 1977). Edge-to-Face (EF) "flocculation" results from the Coulombian attraction between a positive edge and a negative face (Schofield and Samson 1954), and it is well established in thick particles such as kaolinite. Face-to-Face (FF) "aggregation" develops when van der Waals attraction prevails over double layer repulsion (high ionic concentration), and the resulting aggregates have high density. Edge-to-Edge "flocculation" is an intermediate condition between EF flocculation and FF aggregation (at intermediate concentrations).

These observations and supportive experimental evidence permit constructing a fabric map for a soil in terms of the pH and the ionic concentration of the pore fluid. The fabric map for kaolinite is presented in Fig. 2 (evidence and additional details are discussed in Santamarina et al. 2001b).

Groups of associated particles form conglomerates. Conglomerates add a new scale to soil fabric. For example, a soil may involve the edge-to-edge conglomeration of face-to-face associated particles (van Olphen 1977; Bennett and Hulbert 1986). This intermediate scale renders the interpretation of experimental data nonunique. The longer the time sedimenting particles have to agglomerate, the larger the size of the conglomerates and the lower their unit weight. The resulting relationship between density and size suggests a fractal structure (Gregory 1997).

Ultimately, particle associations and conglomerates form the

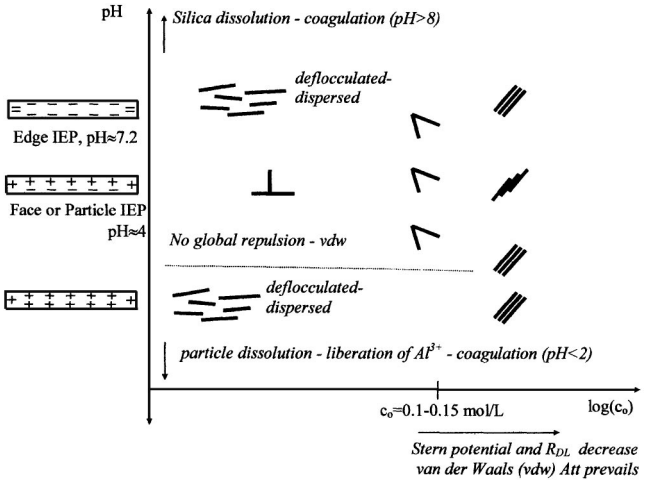

Fig. 2. Postulated particle associations as function of ionic concentration and pH for kaolinite specimens mixed with NaCl electrolytes (modified after Santamarina et al. 2001b)

percolating and stable skeleton that makes a soft soil. However, the relevance of interparticle electrical forces overcomes the skeletal forces until effective stresses reach sufficiently high values (above ~1 kPa for kaolinite and higher for finer soils), at which point a Terzaghian soil forms.

The depth of soft sediments may exceed normal expectations when soil deposits form faster than the rate of pore water dissipation. In this case, hindered settlement or underconsolidation conditions develop. The timescale for the underconsolidation condition depends on the depth and the hydraulic conductivity of the formation (extreme cases, such as the Gulf of Mexico, have timescales that exceed the millennia). Underconsolidation does not imply a soft soil; indeed the impact of the current effective stresses in an underconsolidated deposit may greatly exceed the relevance of electrical forces.

Two additional consequences of the interparticle force balance that governs soft sediments should be considered. First, Terzaghi's principle of effective stress loses relevance, and neither the water content nor the shear strength may be determined by the effective stress, as noted earlier by Zreik et al. (1997). Second, volume change may occur by changing the pore fluid chemistry, which alters the interparticle electrical forces, even when Terzaghi's effective stress is kept constant (Di Maio 1996; Fam and Santamarina 1997).

These micromechanical arguments suggest that the mechanical response of soft sediments is a function of the properties of the particles (e.g., size, mineralogy), the characteristics of the pore fluid (pH, ion type, and concentration), the depth of sediment, and the depositional history. These observations are taken into consideration in the design of the present experimental study.

Scope of the Experimental Study—Selected Clay

The battery of tests conducted in this study involves clay mixed with different ionic concentration fluids to form different soil fabrics. The preliminary sequence of tests includes liquid limit, sedimentation, and viscosity tests. The second sequence of tests is designed to further explore the behavior of soft sediments using low-perturbation elastic and electromagnetic wave-based techniques on specimens with a wide range of water contents. Each test provides additional independent information about soft sediments.

Table 1. Characteristics of Wilkay RP-2 Kaolin

Producer: Wilkinson Kaolin Associates, Gordon, Ga.	
Sieve analysis[a]	
% passing Number 200 sieve	99
coefficient of uniformity, C_u	9.0
coefficient of curvature, C_c	0.67
median particle diameter, d_{50}	3.6×10^{-7} m
Specific surface[b]	21.9 m^2/g
Specific gravity[a]	2.6
GE brightness, % average[a]	78
pH (28% solids), average[a]	5.2
Oil absorption, $g/100$ g clay[a]	40
Minimum dispersed viscosity, 62% solids[a]	4,000+cps
Raw color[a]	cream

[a]Data provided by the manufacturer.

[b]Gas adsorption measurement (Quantachrome NOVA 1200 gas sorption analyzer).

The clay used in all tests is Wilkay RP-2 kaolin. This clay is produced by air flotation, without the addition of chemicals (e.g., dispersants or flocculating agents) during industrial processing. The characteristics of this kaolinite are summarized in Table 1. The excess salts on the kaolinite were determined to be negligible at the ionic concentrations tested. The kaolinite was mixed with the selected NaCl solutions as needed for each test. The selected NaCl solutions were prepared at concentrations: 1×10^{-5}, 4×10^{-4}, 3×10^{-3}, 0.1, and 1.8 mol/L. The complete data set and experimental details can be found in Klein (1999).

Index Tests: Sedimentation, Viscosity, and Liquid Limit

Sedimentation, viscosity, and liquid limit tests can be readily used to gain complementary information about the effects of the pore fluid on the characteristics of sediments, and the relative effects of solids content and remolding. Salient details for these tests follow:

1. Sedimentation tests were conducted on well-mixed specimens prepared at an initial water content of $w=1{,}885\%$, in 1,000 mL graduated cylinders (*ASTM Standard D 422-63*, ASTM 1997b). The sedimentation volume was measured at logarithmic time intervals. The pH and conductivity values of the supernatant fluids of these mixtures were determined after the completion of the test.
2. Viscosity measurements were performed using a Brookfield Digital Viscometer (Model RVDV-E 115) on slurries prepared at three water contents $w=154$, 202, and 257%. Measurements were conducted at 100 rpm without the guard leg. To attain proper resolution, a 14.62 mm diameter spindle was used for the $w=154\%$ specimen and a 27.3 mm diameter spindle was used to test the other specimens.
3. Liquid limit tests were conducted using a Casagrande dish according to *ASTM Standard D 4318-95a* (ASTM 1997a).

Sediment volume is plotted versus time in Fig. 3; from these data, two main parameters are determined: induction time and final sedimentation volume. All test results are summarized in Fig. 4. The following observations can be made:

1. All sedimentation specimens show the typical stages of in-

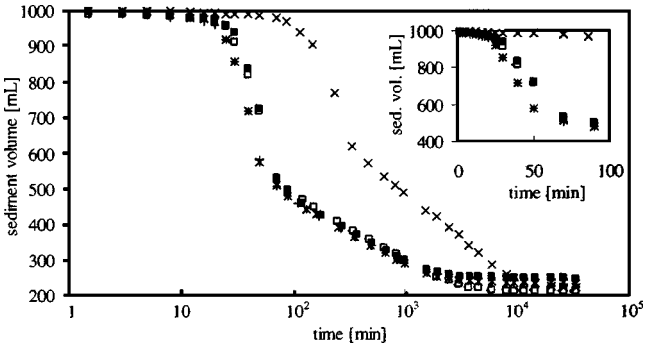

Fig. 3. Sedimentation curve for kaolinite slurries (water content =1885%) with different ionic concentrations: 10^{-5} mol/L (■), 4×10^{-4} mol/L (+), 3×10^{-3} mol/L (*), 0.1 mol/L (□), and 1.8 mol/L (×). Insert highlights initial settlement on linear timescale.

duction, hindered settlement, and consolidation (Fig. 3).

2. The supernatant fluid pH decreases as ionic concentrations increases, suggesting fluid–mineral reactions such as the replacement of H^+ ions by Na^+ ions on the kaolinite surface [Fig. 4(a)]. The conductivity of the supernatant fluid increases linearly with ionic concentration [Fig. 4(d)].
3. Viscosity increases as water content decreases [Fig. 4(f)].
4. Viscosity [Fig. 4(f)], induction time [Fig. 4(b)], and sedimentation volume [Fig. 4(c)] show a minimum around or before the fabric transition ionic concentration $c\sim0.1$ mol/L denoted in Fig. 2.
5. In general, the liquid limit decreases as ionic concentration increases, with an apparent change in trend at around $c\sim10^{-3}$ mol/L (similar results in Warkentin 1961; and in Anson and Hawkins 1998 for $CaCl_2$ solutions). A minimum is not observed near $c\sim0.1$ mol/L [Fig. 4(e)].

Wave-Based Characterization and Monitoring of Soft Sediments

Low energy waves are small perturbations that permit the nondestructive characterization and monitoring of soft sediments. The wave-based characterization and monitoring of soft sediments and slurries has been implemented in previous studies, both in the laboratory during consolidation and triaxial loading (electrical measurements by Mehran and Arulanandan 1977; shear wave measurements by Schultheiss 1981 and Shibuya et al. 1997), and on the seafloor in situ (shear wave measurements by Hamilton et al. 1970; and Hamilton 1971, 1976; Stoll et al. 1988; Richardson et al. 1991). The combined use of elastic and electromagnetic parameters for the simultaneous assessment of triaxial and consolidation tests is documented in Nakagawa et al. (1995) and in Fam and Santamarina (1997).

In this study, wave-based techniques are used to assess kaolinite-water mixtures from the suspension condition to the soil condition, with water contents ranging from $w=0.3$ liquid limit (LL) to $w=9.1$ LL. Data are gathered through three test sequences:

1. High water content ($2.8\ \text{LL}<w<5.4\ \text{LL}$). Measurements

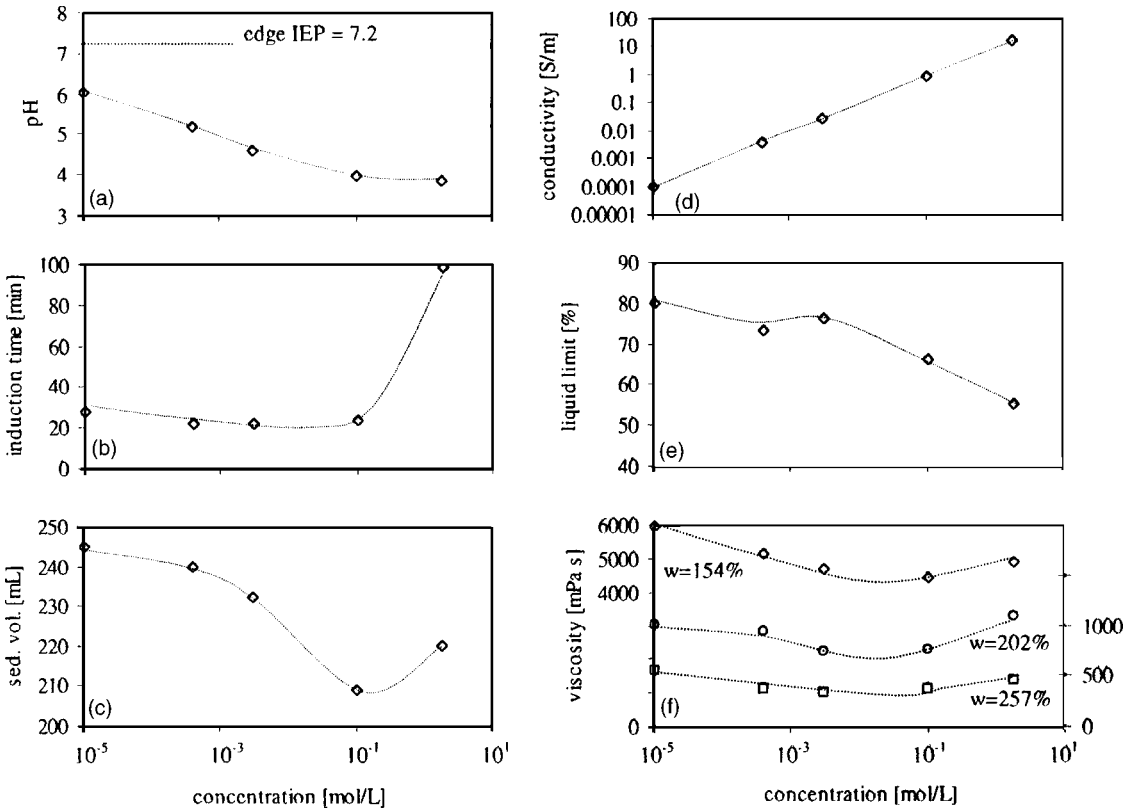

Fig. 4. Index tests—Effect of ionic concentration on: (a) pH of supernatant fluid in sedimentation tests, (b) induction time in sedimentation tests, (c) final sediment volume in sedimentation tests, (d) electrical conductivity of supernatant fluid in sedimentation tests, (e) liquid limit, and (f) viscosity

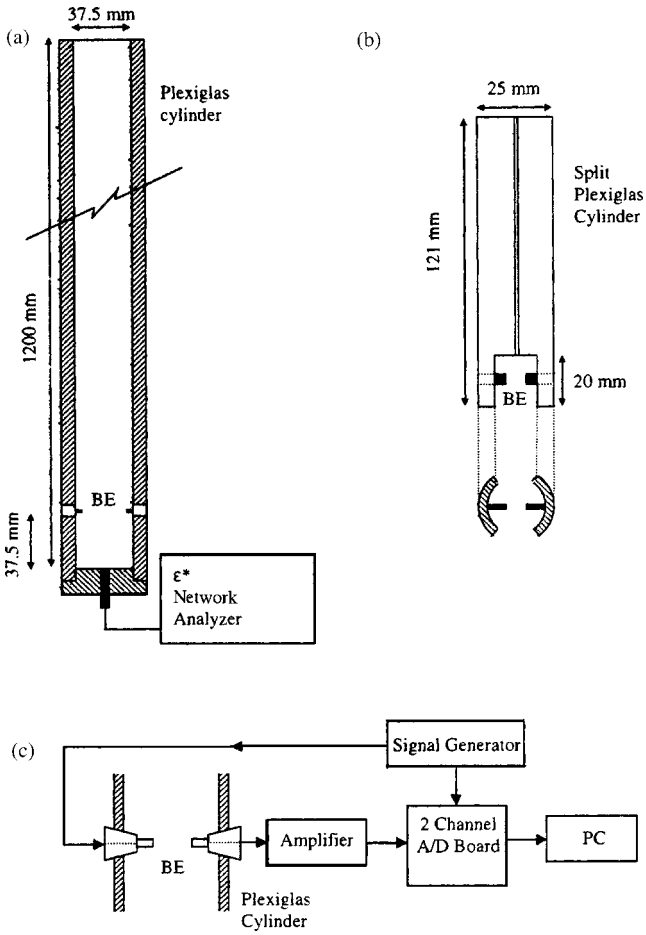

Fig. 5. Test devices: (a) sedimentation column and monitoring transducers and (b) portable S-wave testing device for remolded sediments. Design details: side windows to minimize reflected P-waves, split tube to minimize transmission around tube and global coating with EMI-RFI shield paint and grounding to prevent electrical cross talk. (c) Peripheral electronics for shear wave measurements using bender elements in both devices (shown in *a* and *b*). Note: Complex permittivity is measured with a network analyzer and coaxial probe (as shown in *a*). Equipment specifications are listed in text.

were obtained within a sedimentation column [Fig. 5(a)]. This column incorporates a coaxial termination probe for permittivity measurements at the base of the column. Bender elements for shear wave velocity measurements were placed 37.5 mm above the base of the column.

2. Intermediate water content ($0.7\ \mathrm{LL} < w < 2.3\ \mathrm{LL}$). The intermediate range of water contents could not be attained with high water content mixtures in small sedimentation columns. Therefore, remolded specimens were prepared at predetermined water contents for the different NaCl concentrations, and left for 24 h to allow proper hydration and homogenization prior to testing. While the same coaxial probe was used for permittivity measurements, a hand-held probe with bender elements was developed for these tests [Fig. 5(b)].
3. Low water content ($0.3\ \mathrm{LL} < w < 0.5\ \mathrm{LL}$). In order to explore the broad range of behavior from suspension to soil, an additional dataset was obtained from previously published results. It consists of a similar kaolinite specimen mixed with distilled water. The specimen was mixed at a water content of $w = 100\%$, preconsolidated at 50 kPa gravity loading, and then placed in an oedometer cell instrumented with bender elements and the same coaxial termination probe used in this study.

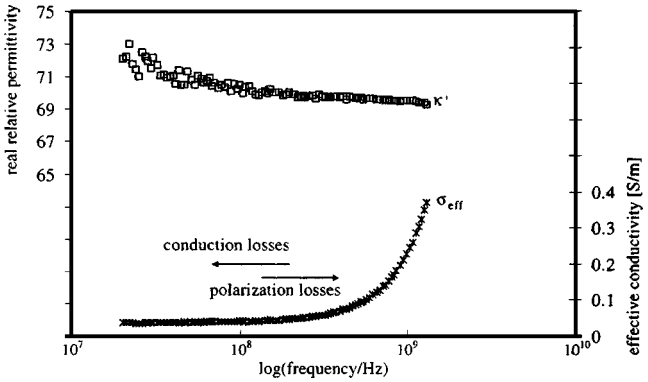

Fig. 6. Permittivity and effective conductivity spectral responses of 3×10^{-3} mol/L specimen 1 min after mixing are presented to facilitate selection of frequencies to be used in discriminating test sequences

The coaxial termination probe (HP-85070A) used to measure the complex permittivity was connected to an HP-8752A network analyzer. Each time a measurement was conducted, spectral data were gathered between 20 MHz and 1.3 GHz. The penetration depth for these measurements is about 3 mm. Peripheral electronics connected to the bender elements included a signal generator (Krohn-Hite 1400A delivering a 5 Hz input step function), preamplifier (Krohn-Hite 3944), and analog to digital (A/D) acquisition system (Rapid System R2000), as shown in Fig. 5(c). The captured signals show the early arrivals of fast P-waves traveling through the mixture (wall reflections). These are removed from the records by low-pass-filtering the signals. Difficulties associated with high conductivity specimens did not permit obtaining a complete data set for the 1.8 mol/L NaCl specimen.

Sample Data and Interpretation Guidelines

The propagation of elastic and electromagnetic waves in soils is affected by distinct soil parameters. Electromagnetic waves excite the charges in the soil, in particular ions and polar water molecules, causing them to displace and to rotate, respectively. The governing soil parameter is the complex relative permittivity κ^*, which consists of real κ' and imaginary κ'' components (the soil used in this study is nonferromagnetic—for a detailed review see Santamarina et al. 2001a)

$$\kappa^* = \kappa' - j\kappa''_{\mathrm{eff}} = \kappa' - j\left(\kappa''_{\mathrm{pol}} + \frac{\sigma}{\varepsilon_0 \omega}\right) = \kappa' - j\frac{\sigma_{\mathrm{eff}}}{\varepsilon_0 \omega} \qquad (1)$$

where $j^2 = -1$ denotes an imaginary number; $\varepsilon_0 = 8.85 \cdot 10^{-12}$ F/m = permittivity of free space; σ = electrical conductivity (S/m); and ω = angular frequency (rad/s). The real part κ' represents the polarizability of the soil and determines the wave velocity, while the imaginary part κ''_{eff} captures conduction and polarization losses. Alternatively, an ac effective conductivity σ_{eff} can be defined by combining the dc conductivity and polarization losses.

Typical real permittivity and effective conductivity spectra are presented in Fig. 6. For reference, spatial and double layer polarizations manifest at MegaHertz frequencies (to the left of the figure), while the relaxation frequency for free water polarization

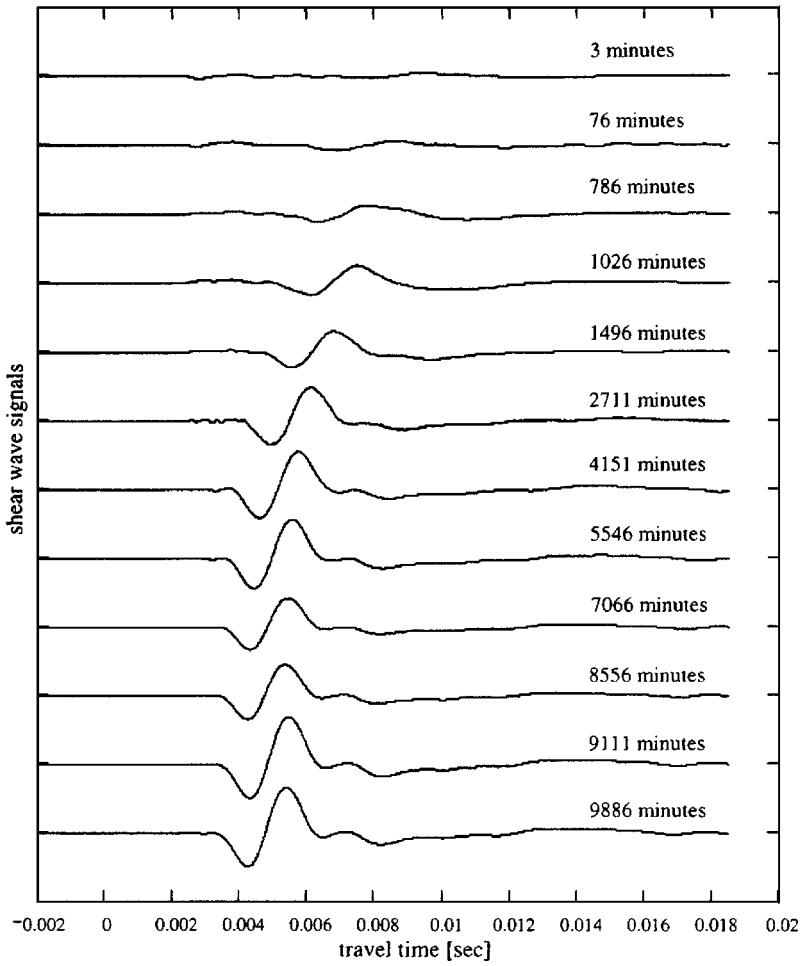

Fig. 7. Evolution of shear waves for kaolinite–electrolyte slurry. This sample data set corresponds to NaCl concentration $= 3 \times 10^{-3}$ mol/L

is about 19 GHz (to the right of the figure). The tails of these polarizations affect the spectral response in the frequency window explored in these measurements. The real relative permittivity shows a minor decrease with increasing frequency, while the effective conductivity is fairly stable at lower frequencies and then increases to reflect free water polarization losses. A preliminary guideline for interpretation is to expect a decrease in real permittivity as the volumetric water content decreases, and an increase in the conductivity of the pore fluid as ionic concentration increases.

On the other hand, the velocity of shear waves through soils is governed by the stiffness of the granular skeleton, which is determined by the forces at interparticle contacts, including both contact-level electrical forces and skeletal forces due to the applied effective stress. For a soil with shear stiffness G and mass density ρ_{mix}, the shear wave velocity is

$$V_s = \sqrt{\frac{G}{\rho_{mix}}} \tag{2}$$

Fig. 7 presents a subset of signatures captured at different times, showing the evolution of shear waves in time for the 3×10^{-3} mol/L specimen. No shear transmission is observed immediately after mixing; however, with time, the amplitude of the signatures begins to increase and the travel time decreases, suggesting the development of a granular skeleton increasingly more capable of transmitting a shear perturbation.

Analysis and Discussion

The experimental results presented previously are herein analyzed in view of questions raised at the outset, placing emphasis on the information that can be gathered from monitoring soft sediments using elastic and electromagnetic waves.

Index Tests and Properties

Viscosity measurements in high water content mixtures reflect hydrodynamic interactions, the differential inertia in particles and fluid, the ensuing interparticle collisions, and the tendency to form different associations as predicted in Fig. 2 or the associated difficulty in dispersing the mixture with the applied shear (Michaels and Bolger 1964; Rand and Melton 1977). In fact, the change in viscosity is one of the most valuable indices for identifying the change from a dispersed to a flocculated fabric when pH decreases below the edge isoelectric point (about pH $\approx$ 7.2 in kaolinite—Fig. 2). Since electrostatic forces in edge-to-face associations are stronger than van der Waals forces in edge-to-edge associations, viscosity decreases as ionic concentration increases [Fig. 4(f)]. The subsequent increase in viscosity with further increase in ionic concentration occurs as the particles form high density face-to-face aggregates that are difficult to break down (Rand and Melton 1977).

The settlement curves for all specimens show an induction

period followed by hindered settlement. The break is not an artifact of the semilog plot, as a pronounced break is also observed in a linear–linear plot (see insert in Fig. 3). The pH of the supernatant fluid in all mixtures is less than the pH at the edge isoelectric point [values plotted in Fig. 4(a)]. For the combined pH and ionic concentration values, the resultant particle associations can be predicted: specimens prepared with $c=10^{-5}$, $c=4\cdot10^{-4}$, and $c=3\times10^{-3}$ mol/L are expected to experience edge-to-face flocculation, the $c=0.1$ mol/L is in a transition condition, and the $c=1.8$ mol/L specimen is expected to develop face-to-face aggregations. Note that a tighter face-to-face aggregation does not imply a higher density sediment [the sedimentation volume increases for the specimen with $c=1.8$ mol/L—Fig. 4(c)]. As indicated earlier, face-to-face aggregated particles may form loose edge-to-face conglomerates; therefore, the mesoscale of conglomerates may hide the trends at the particle scale.

The liquid limit corresponds to the water content at which a saturated, high specific surface soil can withstand a shearing resistance of about 1.7–2.0 kPa. Extensive examples in the geotechnical literature demonstrate that the liquid limit is a function of particle characteristics and fluid composition (Storey and Peirce 1989; Barbour and Yang 1993). Yet, the lack of trend reversal at high ionic concentrations in Fig. 4(e) (which is observed in sedimentation parameters and viscosity), suggests that extensive remolding at high solids contents perturbs interparticle associations, in particular the larger pores that form at the mesoscale of conglomerates (evidence presented in Sridharan et al. 1971; Delage and Lefebvre 1984).

Wave-Based Characterization

Changes in shear wave velocity, real permittivity, and effective conductivity in all of the instrumented sedimentation tests are summarized in Fig. 8. Following the observations made in relation to Fig. 6, the values reported in this summary figure are the real permittivity at 1.3 GHz (to better represent the volumetric free water content without double layer and interfacial polarizations), and the effective conductivity at 0.1 GHz (to avoid free water polarization losses in specimens mixed with low ionic concentration fluids).

The evolution of shear wave velocity is marked by an absence of signals (suspension stage), followed by a region with constant velocity [soft sediment—Fig. 8(a)]. The higher the pore fluid ionic concentration, the higher the initial velocity during the soft sediment stage, yet, all values are very low ($V_s=1$ m/s). Without further evidence, it is hypothesized that the measured velocity in this stage reflects the skeletal stiffness rendered by electrical forces and the ensuing particle associations, in the absence of effective stresses.

The sharp increase in shear wave velocity after about 1,000 min suggests the beginning of the transition from a sediment to a soil, where shear stiffness G gradually becomes determined by the skeletal forces due to the overburden. The water content at which this transition occurs tends to decrease with increasing ionic concentration. This onset of the sediment-to-soil transition appears at a water content that ranges between 3.7 LL and 4.4 LL.

A relationship between the real permittivity and the water content can be established using the complex refractive index analysis (reviewed in Santamarina et al. 2001a), taking into consideration the reduction in permittivity of the pore fluid with ionic concentration

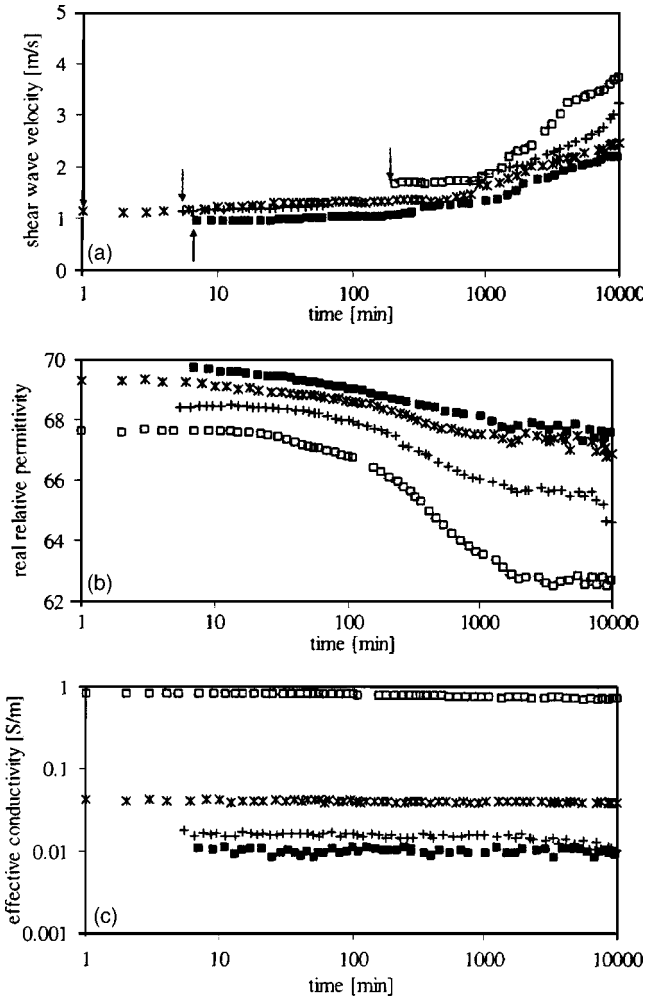

Fig. 8. Evolution of wave parameters during sedimentation of kaolinite–NaCl electrolyte slurries: (a) shear wave velocity—no detectable shear wave signal before arrows, (b) real dielectric permittivity at 1.3 GHz, and (c) effective conductivity at 0.1 GHz. Ionic concentrations are: 10^{-5} mol/L (■), 4×10^{-4} mol/L (+), 3×10^{-3} mol/L (*), and 0.1 mol/L (□)

$$w\% = \frac{\sqrt{\kappa'_{sed}} - 2.65}{\sqrt{(79 - 13\cdot c)} - 2.65}100 \quad \text{(saturated specimens)} \quad (3)$$

where c=ionic concentration of the pore fluid in moles/Liter and κ'_{sed}=real permittivity of the sediment measured at 1.3 GHz. Data in Fig. 8(b) show the decrease in volumetric free water as sedimentation develops; in linear time, the permittivity begins decreasing soon after the test begins. Note that there is an inherent time shift in permittivity and shear wave velocity trends as measurements are taken 37.5 mm apart in the column, as shown in Fig. 5(a) (this separation is needed to minimize wall effects on V_s measurements); however it is expected that errors in interpretation are minimal, given the overall length of the specimen (37.5 versus 1,200 mm).

An expected feature of the conductivity data is the increase in conductivity with the increase in ionic concentration. However, in contrast to the real permittivity, the effective conductivity at 0.1 GHz remains relatively constant throughout this high water content test, even though the volume fraction of electrolyte is decreasing. This observation is further explored next.

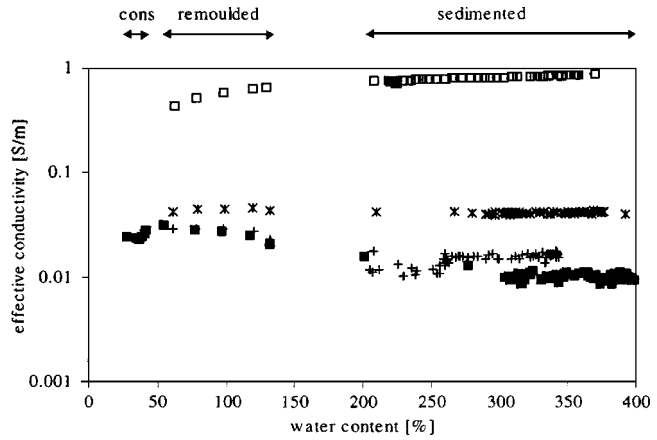

Fig. 9. Variation in effective conductivity at 0.1 GHz as function of gravimetric water content w (estimated from real permittivity κ' measured at 1.3 GHz), for sedimented remolded, and consolidated specimens at four NaCl concentrations: 10^{-5} mol/L (■), 4×10^{-4} mol/L (+), 3×10^{-3} mol/L (*), and 0.1 mol/L (□). Data for consolidated specimens were obtained from Fam and Santamarina (1997) at 0.2 GHz.

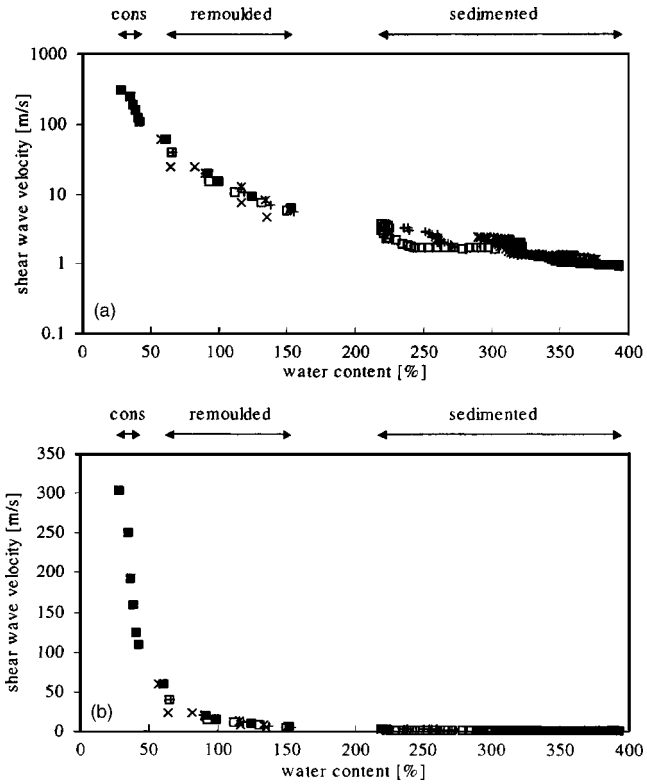

Fig. 10. Change in shear wave velocity as function of gravimetric water content w (estimated from real permittivity κ' measured at 1.3 GHz): (a) log–linear plot to facilitate analysis of low-velocity data; (b) linear–linear plot to identify change in trends. Data correspond to sedimented, remolded and consolidated specimens at five NaCl concentrations: 10^{-5} mol/L (■), 4×10^{-4} mol/L (+), 3×10^{-3} mol/L (*), 0.1 mol/L (□), and 1.8 mol/L (×). Data for consolidated specimens were obtained from Fam and Santamarina (1997).

Broad Water Content Data

The direct relation between the permittivity at 1.3 GHz and the water content captured in Eq. (3) permits plotting effective conductivity data and shear wave velocity data versus local water content for all test data collected in this investigation. This broad water content perspective facilitates the identification of trends that are difficult to perceive otherwise.

Fig. 9 displays effective conductivity data for high (sedimentation), intermediate (remolded), and low (consolidation) water content tests. Two distinct trends become apparent. When the pore fluid has a very low ionic concentration, the displacement of counterions in the double layer (surface conduction) is more important than the conductivity of the electrolyte; then, the lower the water content, the higher the particle content, the higher the contribution of surface conduction, and the higher the conductivity of the mixture (Klein and Santamarina 2003). On the other hand, when the pore fluid has a high ionic concentration, the presence of nonconductive mineral particles takes the place of the more conductive electrolyte; then, the lower the water content, the smaller the amount of electrolyte per volume, and the lower the conductivity. In addition, it is expected that the different fabrics that form at different ionic concentrations render different tortuosities for the flow of ions (Archie 1942; Blewett et al. 2001).

A similar summary plot is presented in Fig. 10 for the shear wave velocity measured in high (sedimentation), intermediate (remolded), and low (consolidation) water content tests. The clear global trend indicates that the stiffness of sediments and soils can be related primarily to water content, with limited effects of the pore fluid characteristics, fabric, and disturbance (e.g., remolding). The changes in shear wave velocity at high water contents are minimal (sedimentation test and part of the remolded tests).

From Suspension to Soft Sediment to Soil

Observations about the properties of the three mixture conditions (suspension, soft sediment, soil) are given in Table 2. Data presented in this paper show that the transition from one condition to the next is affected by the characteristics of the pore fluid.

If the suspension-to-sediment transition is determined by the development of a skeleton with shear stiffness that can support shear wave propagation, then data shown in Fig. 8 suggest that this transition takes place at a water content around 5–7 LL. The suspension-to-sediment transition involves the formation of a percolating, interconnected granular skeleton. Quantities near their percolation threshold follow fractal distributions with respect to size (Sahimi 1994). Therefore, the shear wave velocity at very high water contents near the suspension-to-sediment transition may not be a material constant ($\sim$1 m/s in this study).

The water content at the suspension-to-sediment transition can be compared to that of a flocculated "card castle" structure. A simple geometric analysis renders

$$w\,\% = \frac{\alpha - 1}{2G_s} \cdot 100 \tag{4}$$

where $\alpha = L/d$ = slenderness ratio between the particle length L and its thickness d. This equation highlights the relevance of particle slenderness in soft sediments. The slenderness of kaolinite is about $\alpha = 10$, therefore, the suspension-to-sediment transition should be expected at around $w = 170\% \sim 3$ LL, which is much lower than the observed transition at $w \sim 5-7$ LL. Therefore, granular skeletons formed by small particles when electrical forces prevail can be looser than the card castle structure.

Table 2. Different Soil–Water Conditions

Suspension	Soft sediment	Soil
Interparticle hydrodynamic forces.	Interparticle electrical forces.	Interparticle skeletal forces due to applied effective stress at boundaries.
No skeleton.	There is a percolating granular skeleton. Its properties are determined by electrical forces.	The shear strength, stiffness and volume change behavior are determined by the applied effective stresses.
No shear stiffness.	The shear stiffness is independent of the effective stress.	The shear stiffness depends on the effective stress.
Particle interaction may develop through long-range hydrodynamic effects (may affect viscosity).	Fabric is determined by long-range electrical forces. Particle associations and conglomerates develop. Fabric affects the properties of the medium.	Mesoscale conglomerates are distorted during remolding.
No time effects (refers to very small or buoyant-particles).	Thixotropic effects at constant volume (or quasi) can be very relevant.	Thixotropy and chemical–mechanical coupling effects gradually vanish as effective confinement increases and porosity decreases.

The slenderness of montmorillonite particles may reach $\alpha = 100$, therefore, the sediment-to-soil transition should occur at water contents greater than ~1900%. However, the potential for edge-to-face association in montmorillonite is questionable (Secor and Radke 1985), and an experimental determination is required.

A clear criterion for the sediment-to-soil transition is lacking. The onset in the change in shear stiffness observed in the sedimentation tests (Fig. 8—water content between 3.7 and 4.4 LL) is not apparent when all the available data are combined and plotted in log–log scale in Fig. 10(a) (the log–log scale facilitates the comparative analysis of small velocities). When data are plotted in linear–linear scale [Fig. 10(b)], a definite transition appears at $w \sim 1-3$ LL. This transition agrees with the sediment-to-soil transition water content previously observed by Fakher et al. (1999) (kaolin and sandy silty clays—large strain test viscometer). In any case, the progression from prevailing electrical forces to prevailing skeletal forces obscures this transition.

Unless other forces develop (such as suction), the "soft sediment" layer above the soil layer in Fig. 1 is permanent. That is, the soft sediment-to-soil transition may never occur at small depths (Michaels and Bolger 1962). The depth to which electrical forces prevail over skeletal forces depends on the unit weight of the soft sediment and the particle size, as shown in Fig. 11. For micron size particles, the thickness of the soft sediment layer is on the order of centimeters, while it may reach several meters in montmorillonite.

Conclusions

Three high water content conditions are identified: suspension ($\sigma' = 0$ and $G = 0$), soft sediment ($\sigma' = 0$ and $G > 0$), and soil ($\sigma' > 0$ and $G > 0$). At the macroscale, soft sediments are high water content saturated deposits made of clay-size particles subjected to low effective confinement. At the particle level, soft sediments consist of a granular skeleton formed by grains with diameters less than ~10 μm, in the absence of interparticle capillary forces, and where interparticle electrical forces are relevant relative to the skeletal forces that result from the applied effective stress.

Liquid limit, sedimentation, and viscosity measurements reflect variations in soil fabric due to changes in ionic concentration. For the tested kaolinite mixtures (pH < edge isoelectric point; very low to high ionic concentrations), data from sedimentation and viscosity tests suggest that significant fabric changes occur in the soil around $c \sim 0.1$ mol/L. This observation is supported by published studies for kaolinite, which show that edge-to-face flocculation takes place at low ionic concentrations, while face-to-face aggregates form at high ionic concentrations. The liquid limit test is a high solids content test with extensive remolding, hence, it is less sensitive to fabric effects than viscosity or sedimentation tests.

High frequency permittivity is a good indicator of water content, and can be effectively used to monitor the evolution of high water content mixtures. The effective conductivity increases as porosity increases for high ionic concentration fluids. The opposite is true for low ionic concentration fluids due to the contribution of surface conduction.

The maximum porosity a soft sediment may attain is determined by the particle slenderness. In the case of kaolinite, a skel-

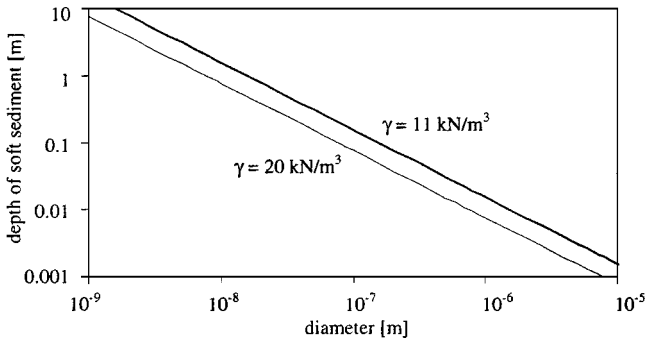

Fig. 11. Depth of soft sediment that can form under condition that electrical forces are greater than interparticle skeletal forces. Analysis includes van der Waals forces and gravitational forces, and assumes spherical particles. Thickness is computed for two total unit weights of soft sediment: 11 and 20 kN/m^3.

eton capable of transmitting a shear perturbation is observed at a water content as high as six times the liquid limit, which corresponds to a fabric significantly looser than a card-castle structure. At this incipient skeletal condition, minor differences in shear wave velocity hint at the stiffness of different fabrics.

In a wide range of water contents ($0.6\ LL < w < 6\ LL$), the shear wave velocity is primarily determined by the water content or porosity, and fabric appears to have a limited impact. Shear wave velocities as low as 1 m/s are observed in soft kaolinite sediments.

Shear wave velocity appears to be a good measurement of a wide range of conditions, and an indicator of the transitions from one regime to the next. The "suspension" condition is denoted by the absence of shear waves. The appearance of shear waves indicates the suspension-to-soft sediment transition. Finally, the increase in shear wave velocity with effective confinement suggests the formation of a "Terzaghian soil."

In summary, the mechanical response of soft sediments is a function of the properties of the particles (e.g., size, mineralogy), the characteristics of the pore fluid (pH, ion type, and concentration), the depth of sediment, and the depositional history.

Test procedures and interpretation guidelines developed in this study can be used to design parallel tools for the field characterization of soft sediments, dredging operation optimization, and foundation scour risk assessment; for quality control related to drilling mud, hydraulic fill, or flowable fill; and for monitoring mining processes such as separation tanks, waste disposal, and tailing ponds.

Acknowledgments

Support for this research was provided by the Georgia Mining Industry, NSF-USA, NSERC-Canada, and The Goizueta Foundation.

References

American Society for Testing and Materials (ASTM). (1997a). "Standard test method for liquid limit, plastic limit, and plasticity index of soils." *Designation: D 4318-95a, 1997 Annual book of ASTM standards*, Vol. 04.08, Philadelphia, 522–532.

American Society for Testing and Materials (ASTM). (1997b). "Standard test method for particle-size analysis of soils." *Designation: D 422-63, 1997 Annual book of ASTM standards*, Vol. 04.08, Philadelphia, 10–16.

Anson, R. W. W., and Hawkins, A. B. (1998). "The effect of calcium ions in pore water on the residual shear strength of kaolinite and sodium montmorillonite." *Geotechnique*, 48, 787–800.

Archie, G. E. (1942). "The electrical resistivity log as an aid in determining some reservoir characteristics." *Trans. Am. Inst. Min., Metall. Pet. Eng.*, 146, 54–62.

Barbour, S. L., and Yang, N. (1993). "A review of the influence of clay-brine interactions on the geotechnical properties of Ca-montmorillonitic clayey soils from western Canada." *Can. Geotech. J.*, 30, 920–934.

Been, K., and Sills, G. (1981). "Self-weight consolidation of soft soils: an experimental and theoretical study." *Geotechnique*, 31, 519–535.

Bennett, R. H., and Hulbert, M. H. (1986). *Clay microstructure*, Geological Sciences Series, International Human Resources Development Corporation, Boston.

Blewett, J., McCarter, W. J., Chrisp, T. M., and Starrs, G. (2001). "Technical note: Monitoring sedimentation of a clay slurry." *Geotechnique*, 51, 723–728.

Delage, P., and Lefebvre, G. (1984). "Study of the structure of a sensitive Champlain clay and of its evolution during consolidation." *Can. Geotech. J.*, 21, 21–35.

Di Maio, C. (1996). "Exposure of bentonites to salt solution: osmotic and mechanical effects." *Geotechnique*, 46(4), 695–707.

Esquivel-Sirvent, R., Green, D. H., and Yun, S. S. (1995). "Critical mechanical behaviour in the fluid/solid transition of suspensions." *Appl. Phys. Lett.* 67, 3087–3089.

Fakher, A., Jones, C., and Clarke, B. (1999). "Yield stress of super soft clays." *J. Geotech. Geoenviron. Eng.* 125, 499–509.

Fam, M., and Santamarina, J. C. (1997). "A study of consolidation using mechanical and electromagnetic waves." *Geotechnique*, 47, 203–219.

Gregory, J. (1997). "The density of particle aggregates." *Water Sci. Technol.* 36, 1–13.

Hamilton, E. L. (1971). "Elastic properties of marine sediments." *J. Geophys. Res.*, 76, 579–604.

Hamilton, E. L. (1976). "Shear-wave velocity versus depth in marine sediments: A review." *Geophysics* 41, 985–996.

Hamilton, E. L., Bucker, H. P., Keir, D. L., and Whitney, J. A. (1970). "Velocities of compressional and shear waves in marine sediments determined in situ from a research submersible." *J. Geophys. Res.*, 75, 4039–4049.

Inoue, T., Tan, T.-S., and Lee, S.-L. (1990). "An investigation of shear strength of slurry clay." *Soils Found.*, 30, 1–10.

Israelachvili, J. (1992). *Intermolecular and Surface Forces*, Academic, New York.

Klein, K. A. (1999). "Electromagnetic properties of high specific surface minerals." PhD dissertation, Georgia Institute of Technology, Atlanta.

Klein, K., and Santamarina, J. C. (2003). "Electrical conductivity in soils: Underlying phenomena." *J. Environ. Eng. Geophysics*, 8(4), 263–273.

Kynch, G. J. (1952). "A theory of sedimentation." *Trans. Faraday Soc.* 48, 166–176.

Lyklema, J. (1995). *Fundamentals of interface and colloid science*, Vol. II, Academic, New York.

McRoberts, E. C., and Nixon, J. F. (1976). "A theory of soil sedimentation." *Can. Geotech. J.*, 13, 294–310.

Mehran, M., and Arulanandan, K. (1977). "Low frequency conductivity dispersion in clay-water-electrolyte systems." *Clays Clay Miner.*, 25, 39–48.

Michaels, A. S., and Bolger, J. C. (1962). "Settling rates and sediment volumes of flocculated kaolin suspensions." *Ind. Eng. Chem. Fundam.*, 1, 24–33.

Michaels, A. S., and Bolger, J. C. (1964). "Particle interactions in aqueous kaolinite dispersions." *Ind. Eng. Chem. Fundam.*, 3, 14–20.

Mitchell, J. K. (1993). *Fundamentals of soil behaviour*, 2nd Ed., Wiley, New York.

Nakagawa, K., Soga, K., Mitchell, J. K., and Sadek, S. (1995). "Soil structure changes during and after consolidation as indicated by shear wave velocity and electrical conductivity measurements." *Compression and consolidation of clayey soils*, H. Yoshikuni and O. Kusakabe, eds., Balkema, Rotterdam, The Netherlands, 1069–1074.

Rand, B., and Melton, I. E. (1977). "Particle interactions in aqueous kaolinite suspensions I. Effect of pH and electrolyte upon the mode of particle interaction in homoionic sodium kaolinite suspensions." *J. Colloid Interface Sci.* 60, 308–320.

Richardson, J. F., and Zaki, W. N. (1954). "Sedimentation and fluidisation: Part I." *Trans. Inst. Chem. Eng.*, 32, 35–53.

Richardson, M. D., Muzi, E., Troiano, L., and Miaschi, B. (1991). "Sediment shear waves: A comparison of in situ and laboratory measurements." *Microstructure of fine-grained sediments, from mud to shale*, Bennett, Bryant, and Hulbert, eds., Springer, New York, 403–415.

Sahimi, M. (1994). *Applications of percolation theory*, Taylor & Francis, Bristol, U.K.

Santamarina, J. C. (2003). "Soil behavior at the microscale: Particle forces." *Proc., Soil Behavior and Soft Ground Construction—The Ladd Symp.*, Vol. 119, ASCE and the Geo-Institute, New York, 25–56.

Santamarina, J. C., Klein, K., and Fam, M. (2001a). *Soils and waves*, Wiley, Chichester, U.K.

Santamarina, J. C., Klein, K., Palomino, A., and Guimaraes, M. (2001b). "Microscale aspects of chemical-mechanical coupling: Interparticle forces and fabric." *Chemo-mechanical coupling from nano-structure to engineering applications*, Di Maio, Hueckel, and Loret, eds., Maratea, Italy, 47–64.

Schofield, R. K., and Samson, H. R. (1954). "Flocculation of kaolinite due to the attraction of oppositely charged crystal faces." *Discuss. Faraday Soc.* 18, 135–145.

Schultheiss, P. J. (1981). "Simultaneous measurement of P & S wave velocities during conventional laboratory soil testing procedures." *Mar. Geotech.*, 4, 343–367.

Secor, R. B., and Radke, C. J. (1985). "Spillover of the diffuse double layer on montmorillonite particles." *J. Colloid Interface Sci.* 103, 237–244.

Shibuya, S., Hwang, S. C., and Mitachi, T. (1997). "Elastic shear modulus of soft clays from shear wave velocity measurements." *Geotechnique*, 47, 593–601.

Sposito, G. (1998). "On points of zero charge." *Environ. Sci. Technol.* 32, 2815–2819.

Sridharan, A., Altschaeffle, A. G., and Diamond, S. (1971). "Pore size distribution studies." *J. Soil Mech. Found. Div.*, 97(5), 771–787.

Sridharan, A., and Prakash, K. (1998). "Characteristic water contents of a fine-grained soil-water system." *Geotechnique*, 48, 337–346.

Stoll, R. D., Bryan, G. M., Flood, R., Chayes, D., and Manley, P. (1988). "Shallow seismic experiments using shear waves." *J. Acoust. Soc. Am.*, 83, 93–102.

Storey, J. M. E., and Peirce, J. J. (1989). "Influence of changes in methanol concentration on clay particle interactions." *Can. Geotech. J.*, 26, 57–63.

Tiller, F. M., and Khatib, Z. (1984). "The theory of sediment volumes of compressible, particulate structures." *J. Colloid Interface Sci.*, 100, 55–67.

Toorman, E. (1999). "Sedimentation and self-weight consolidation: constitutive equations and numerical modelling." *Geotechnique*, 49, 709–726.

van Olphen, H. (1977). *Clay colloid chemistry*, Krieger, Malabar, Fla.

Velde, B. (1992). *Introduction to clay minerals—Chemistry, origins, uses and environmental significance*, Chapman and Hall, New York.

Warkentin, B. P. (1961). "Interpretation of the upper plastic limit of clays." *Nature (London)*, 190, 287–288.

Weaver, C. E. (1989). *Clays, muds, and shales*, Elsevier, New York.

Williams, D. J. A., and Williams, K. P. (1978). "Electrophoresis and zeta potential of kaolinite." *J. Colloid Interface Sci.* 65, 79–87.

Work, L. T., and Kohler, A. S. (1940). "Sedimentation of suspensions." *Ind. Eng. Chem.* 32, 1329–1334.

Zreik, D., Germaine, J., and Ladd, C. (1997). "Undrained strength of ultra-weak cohesive soils: Relationship between water content and effective stress." *Soils Found.*, 37, 117–128.